Influence of Various Structural Factors of Claw Pole Transverse Flux Permanent Magnet Machines on Internal Voltage using Finite Element Analysis

Ali Alaeddini[1], Ahmad Darabi[1], Hamed Tahanian[1]

Abstract: This paper presents the influence of several structural factors and parameters involved in the design of Claw Pole Transvers Flux Permanent Magnet Machines (TFPMs) on their internal voltage. Knowing the influence of each factor is very important for an effective process of design and optimization for these machines. In this paper by using the complete design algorithm of Claw Pole TFPM, only one parameter is changed at a time and its influence on the internal voltage is analyzed. Output torque is also studied, because the internal voltage has effect on both the average and the ripple of output torque. The most important factors and parameters which are considered are: 1) number of poles; 2) length of air gap; 3) ratio of magnet arc to flux concentrator arc in each pole of rotor; 4) shape of pole shoe of stator and 5) area of rotor pole covered by stator pole. Due to geometrical complexities of TFPMs, analytical methods fail to describe the behavior of these machines. For this reason, in this paper finite element analysis is used both in the design and analysis of TFPMs.

Keywords: Claw pole transverse flux permanent magnet machine, Design optimization, Finite element analysis, Internal voltage, Output torque.

1   Introduction

Transverse Flux Permanent Magnet machines (TFPMs) are widely used in electrical propulsion systems, because of their efficiencies and high power and torque densities [1]. Unlike conventional machines, electromagnetic torque in transverse flux machines is proportional to the number of poles [2]. Because of this unique feature, the torque density of these machines could be increased up to several times of conventional machines by increasing the number of poles. As the mass and volume of electric machines are dependent on their nominal torque, this unique feature of TFPM machines is used in low speed applications, such as wind power generators and marine propulsion motors, where access to high torque density is critical [2 – 4].

---

[1]Faculty of Electrical Engineering, University of Shahrood, Shahrood, Iran;
 E-mails: alaeddini.ali@gmail.com, darabi_ahmad@hotmail.com, ha_tahanian@yahoo.com

TFPM machine was introduced by Weh in 1986 [5]. Since then on, several topologies have been proposed for TFPMs which can be classified into two major categories: 1) the double-sided topologies with high-power production capabilities, but complicated structures and 2) the single-sided topologies with lower power production capabilities, but simpler structures [6]. Compared to other TFPM topologies, the claw pole TFPM benefits from the simplicity of the single-sided TFPMs, while its performance is comparable with double-sided ones [7].

Based on Waveform of the internal voltage, all permanent magnet motor drives are classified into two major categories: 1) the permanent magnet synchronous motor (PMSM), which has a sinusoidal internal voltage and requires sinusoidal stator currents to produce constant torque, and 2) the brushless dc motor (BDCM), which has a trapezoidal internal voltage and requires rectangular stator currents to produce constant torque [8]. So if the transverse flux permanent magnet machines are used as PMSM, the internal voltage should be close to a pure sine wave. While if they are used as BLDC, the internal voltage should be as trapezoid.

In addition, the internal voltage waveform has influence on both the average and the ripple of electromagnetic torque. There have been extensive efforts to reduce ripples of electromagnetic torque to improve the quality of electrical machines performance. Ripples of electromagnetic torque are mostly the main sources of noise and vibration of electrical machines [9]. Therefore, due to usage of TFPMs in high torque applications, special attention should be paid to the internal voltage waveform of machine in the process of design and optimization.

There are several parameters and structural factors which are effective on the internal voltage of Claw Pole TFPMs. The most important factors and parameters which are considered are: number of poles, length of air gap, ratio of magnet arc to flux concentrator arc in each pole of rotor, shape of pole shoe of stator, and area of rotor pole covered by stator pole.

2 Structure and Design of Claw Pole TFPM

2.1 Claw pole TFPM structure

Fig. 1 is one pole pair of one phase of a claw pole TFPM designed in this paper. In this figure only active materials (include of stator core back, ring winding, stator teeth, flux concentrators and permanent magnets) of machine are illustrated. One phase is constructed by putting together these pole pairs around the axis of motor. As this figure shows, the stator consists of a back core and claw teeth which enclose the armature winding. The basic dimensions of the claw pole TFPM machines are illustrated in Fig. 2. These dimensions are listed in **Table 1**.
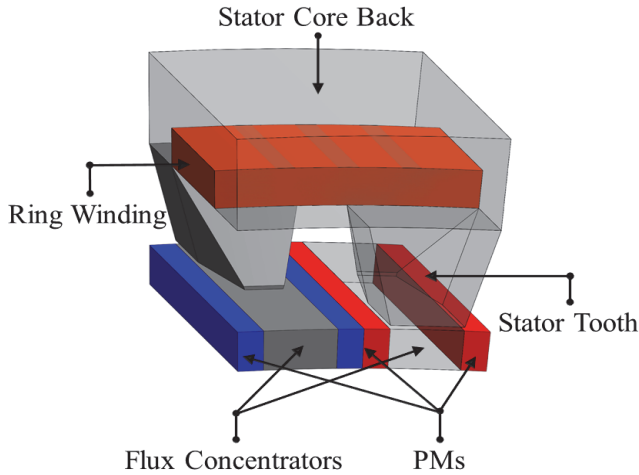
Fig. 1 – *One pole pair of one phase of the claw pole TFPM.*

For the most of the multi-phase TFPM machines, each phase is designed and built individually as a single phase machine and then a number of single phase machines are assembled on a common shaft to present a multi-phase machine. By the other words, for designing a P kW, m-phase machine, where m is the number of phases, it would be required to design m identical single phase machines with the rating of each is equal to P/m kW. Multi-phase structure is achieved by stacking shifted phases along the machine axis direction. In order to reach smooth torque, the phases have to be shifted by 360/m electrical angle. This phase shift can either be applied to stator teeth or rotor elements. It is stated in [6] that when stator teeth of adjacent phases are shifted and rotor elements are aligned, cogging torque amplitude is lower than other combinations.
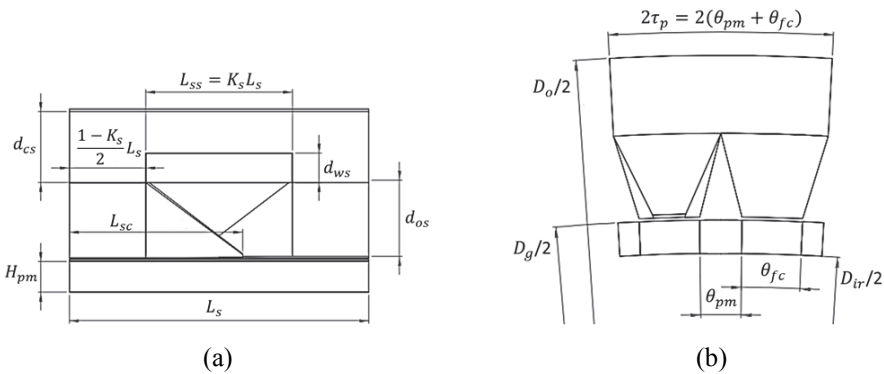

(a)   (b)

Fig. 2 – *Main sizing parameters of Claw Pole TFPM machine:* (a) *Side view,* (b) *Front view.*

Table 1
Case study ratings and parameters.

Symbol	Quantity	Value
P	rated power	500 kW
n_s	rated speed	300 rpm
f	rated frequency	300 Hz
p	number of pole pairs	60
V_m	maximum available phase voltage amplitude	105 V
m	number of phases	6
B_g	average flux density in air gap	0.3529 T
B_m	flux density of PM at operating point	0.8994 T
g	air gap length	1 mm
D_o	outer diameter	1292 mm
D_{ir}	inner diameter	1182 mm
D_g	air gap surface diameter	1200 mm
d_{ws}	redial length of stator slot	12.5 mm
d_{cs}	thickness of stator core back	12 mm
d_{os}	length of stator tooth	21.5 mm
H_{pm}	redial length of PMs	8 mm
L_s	axial length of each phase	100 mm
L_{ss}	slot axial length	43 mm
K_s	ratio of the slot axial length	0.43
K_{co}	ratio of the stator pole area to rotor pole area	0.5
K_m	ratio of magnet arc to flux concentrator arc	0.7
K_{lpm}	PM leakage coefficient	0.24
K_{lt}	stator tooth leakage coefficient	0.0066

2.2 Claw Pole TFPM design

For this paper, design of Claw Pole TFPM is based on the sizing equations of [1, 7, 10]. However, it is better to use more accurate equations to calculate some dimensions of Claw Pole TFPMs. Length of stator tooth d_{os} is calculated by

$$d_{os} = \frac{D_g}{2}\left[\frac{2K_{co}(1-K_{lt})}{(1-K_s)(1+K_m)} - 1\right], \tag{1}$$

where D_g is the air gap surface diameter, K_s is the ratio of the slot axial length L_{ss} over the axial length of each phase L_s, K_m ratio of magnet arc to flux concentrator arc in each pole of rotor, and K_{co} is the ratio of the area of rotor pole covered by stator pole to the area of the rotor flux concentrator. K_{lt} is factor

related to flux leakage in stator teeth which is determined by using finite element analysis. To reduce the leakage flux between adjacent stator teeth, a minimum value for d_{os} is selected which is given by

$$d_{os,\min} = \frac{L_s}{2}(2K_{co} + K_s - 1),\tag{2}$$

Therefore, if value of d_{os} from (1) is lower than $d_{os,\min}$, length of stator tooth is selected to be $d_{os,\min}$.

Thickness of stator core back d_{cs} is given by

$$d_{cs} = \frac{(1 - K_s)[(D_g/2) + d_{os}]L_s}{4[(D_g/2) + d_{os} + d_{ws}]},\tag{3}$$

where d_{ws} is the radial length of stator slot. The other important dimension is the radial length of permanent magnets H_{pm} which is calculated by

$$H_{pm} = \frac{\pi B_g D_g}{4p(1 - K_{lpm})B_m},\tag{4}$$

where B_g is the average flux density in air gap, p is the number of pole pairs, B_m is the flux density of permanent magnet at their operating point, K_{lpm} is a factor related to flux leakage of permanent magnets (flux of PMs which doesn't enter the stator teeth) and K_{lpm} is determined like K_{lt}.

2.3 Parameters and materials of the case study

For investigation of structural parameters effects which are considered in this paper, complete design algorithm of Claw Pole TFPM is used. A 6-phase, 500 kW claw pole transverse flux permanent magnet machine is selected as the case study. One phase designed claw pole TFPM motor is depicted in Fig. 3. Its maximum available phase voltage amplitude with 300 Hz frequency is 105 V. This high power motor is designed for marine electric propulsion systems, where available source voltage is very low in amplitude. Therefore, the amplitude of phase current is very high. This is not a problem, since for a low voltage machine the number of stator winding turns is low (for the case study is 1 turn per phase). Also, the area of the stator slot in TFPM machines is calculated by the maximum allowed current density of the winding and not by the amplitude of phase current. However, this area could be selected easily as large as enough for placement of winding (for example by increasing the d_{ws} in Fig. 2a). Structural parameters studied in this paper are showed in **Table 1**. In design process, only one parameter is changed at a time while other parameters remained constant and by considering these conditions, the influence of that

parameter on the internal voltage is analyzed. Materials which have been used in the structure of motor are given in **Table 2**.

Since the case study motor is employed where only 3-phase source is available, it should have been designed with 3 phases. However, because of the outer diameter limit, 6 phases should be connected together in order to provide the required output power of 500 kW. It should be noted that it is possible to build a 6-phase system using a 3-phase system. The 6-phase claw pole TFPM motor is depicted in Fig. 4.

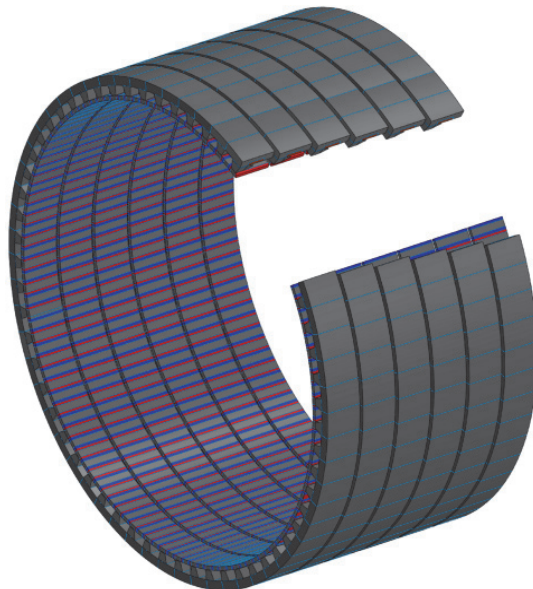**Fig. 3 –** *Part of one phase of designed claw pole TFPM motor.*

Fig. 4 – *Six phase designed claw pole TFPM motor.*

Table 2

Materials employed in the structure of case study motor.

Part of machine	Material
stator core	Somaloy500+0.5%Kenolube_800MPa
rotor flux concentrators	Somaloy500+0.5%Kenolube_800MPa
permanent magnets	NEOMAX-32EH
armature winding	Copper

3 Investigation of Structural Parameters Effects on Internal Voltage and Output Torque Ripple

Because of complex structure of the claw pole TFPM machine, several parameters and structural factors extremely impact on machine performance. Considering that the performance of a TFPM machine is mainly dependent on the internal voltage, its studying is necessary for investigating of the structural parameters dependence on the machine performance. Waveforms of the internal voltage, hence its harmonic content, depends on the structure and constructive materials of the machine and the level of core saturation.

One of the most important criteria for judging the impact of structural factors on the internal voltage waveform and performance of TFPM machine is electromagnetic torque. Therefore, due to usage of TFPMs in high torque applications, special attention should be paid to the internal voltage waveform of the machine in both the design and optimization process. In these applications, the machine should have high torque density while its torque ripple, should be minimal.
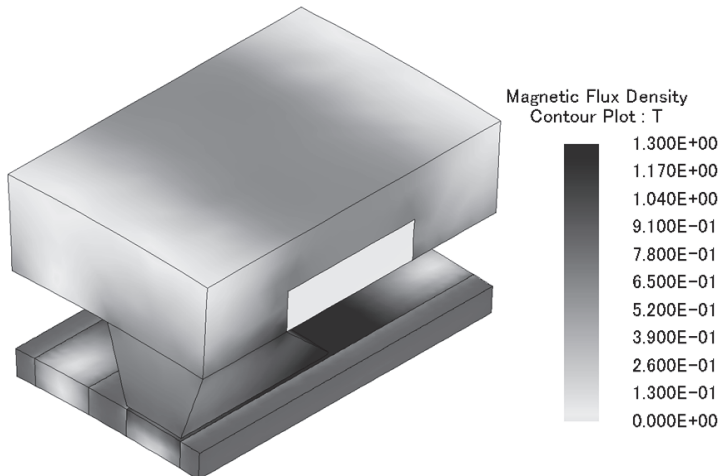

Fig. 5 – *Flux density distribution of one pole pair at open circuited operating condition.*

In this section, the influence of different structural factors and parameters on the internal voltage and the output torque waveforms is studied. For this purpose, only one parameter of the case study varies while the other parameters are kept constant. For each value of the variable parameter a new machine is designed by using the complete design algorithm.

Fig. 5 shows flux density distribution of the motor for the time $t = 0$ at open circuited operating condition. $t = 0$ is chosen as a time when the flux linkage of phase 'a' is minimum and hence, the relevant internal voltage is zero.

Due to the lack of electromagnetic coupling between the phases, the waveform of each phase internal voltage is independent of the number of phases. Values of flux linkage at 48 steps under open circuit condition for the case study are obtained by a finite element analysis carried out using JMAG Designer 10.5 [11]. Internal voltage of each phase is calculated as time derivative of flux linkage of the relevant phase winding at open circuited condition. For an m-phase machine, the internal voltage en of phase n is written as

$$e_n(\omega_e t) = \sum_{h=1}^{\infty} E_h \cos\left[h\omega_e t - h(n-1)\frac{2\pi}{m} + \theta_{eh} \right], \quad n = 1, 2, 3, ..., m, \quad (5)$$

in which ω_e, h, E_h and θ_{eh} are the fundamental electric angular frequency, the harmonic order, the amplitude of h-th harmonic of internal voltage, and the h-th harmonic phase angle of internal voltage, respectively.

Having internal voltages, self-inductances and resistances of all phases, phase currents of the motor is obtained at each load through a simulation of dynamic transient model of the machine. Current of phase n of an m-phase machine could be written as

$$i_n(\omega_e t) = \sum_{k=1}^{\infty} I_k \cos\left[k\omega_e t - k(n-1)\frac{2\pi}{m} + \theta_{ik} \right], \quad n = 1, 2, 3, ..., m, \quad (6)$$

where k, I_k and θ_{ik} are the harmonic order of phase current, the amplitude of k-th harmonic of phase current, and the k-th harmonic phase angle of phase current, respectively.

The electromagnetic torque is expressed in terms of internal voltage and phase current waveforms by using Fourier series. Instantaneous electromagnetic torque Te is defined as

$$T_e = \frac{\sum_{n=1}^{m} e_n i_n}{\omega_r}, \quad (7)$$

where ω_r is the angular speed of rotor. In steady state, ω_r is constant. Substitution of (5) and (6) into (7) results in

136

$$T_e\left(\omega_e t\right) = \frac{1}{\omega_r} \sum_{n=1}^{m} \left\{ \sum_{h=1}^{\infty} E_h \cos\left[h\omega_e t - h\left(n-1\right)\frac{2\pi}{m} + \theta_{eh} \right] \right.$$
$$\left. \times \sum_{k=1}^{\infty} I_k \cos\left[k\omega_e t - k\left(n-1\right)\frac{2\pi}{m} + \theta_{ik} \right] \right\}. \tag{8}$$

Calculation of the instantaneous electromagnetic torque can be done using (8) for the case study.

3.1 The influence of number of poles

One of features of the claw pole TFPM machine is that the number of poles can be increased without reducing the cross section of the coil, which leads to higher torque density [12]. Theoretically, this definition implies that a claw pole TFPM machine with infinite output power will be achievable. For the higher pole numbers, 1) the distance between adjacent stator teeth is reduced, and 2) saturation will be higher than usual because cross sectional area of the flux per pole is reduced while core flux density is remained constant. These two effects will cause the increased leakage flux in the claws. Therefore, increasing the number of poles is limited due to the increase of flux leakage. In addition, there are some mechanical constraints in terms of manufacturability [13]. In this section, the effect of number of poles on operation of the claw pole transverse flux permanent magnet machine at a constant frequency (variable speed) will be discussed. In Fig. 6 the effect of the number of poles on the internal voltage at constant frequency is shown. As is clear from this Figure, by reducing the number of poles at constant frequency, internal peak voltage becomes sharper, which means that the internal voltage waveform is more far from a pure sine waveform. Considering Fig. 7 output torque ripple has decreased from 157.05% for 10 poles machine to 22.47% for 60 poles machine.
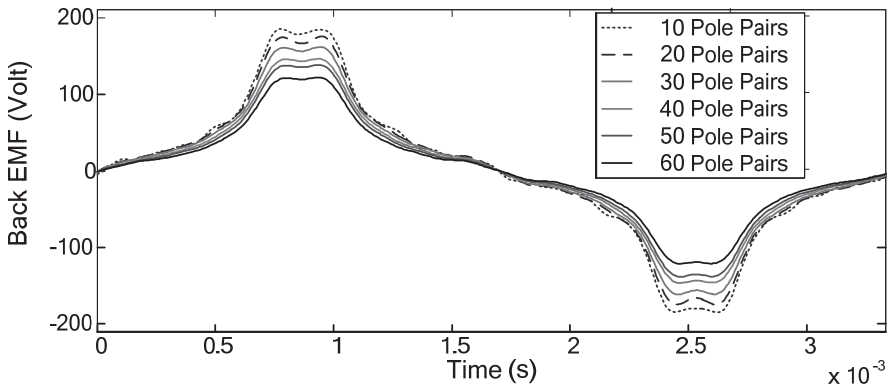

Fig. 6 – *Internal voltage waveform for different pole numbers at constant frequency.*
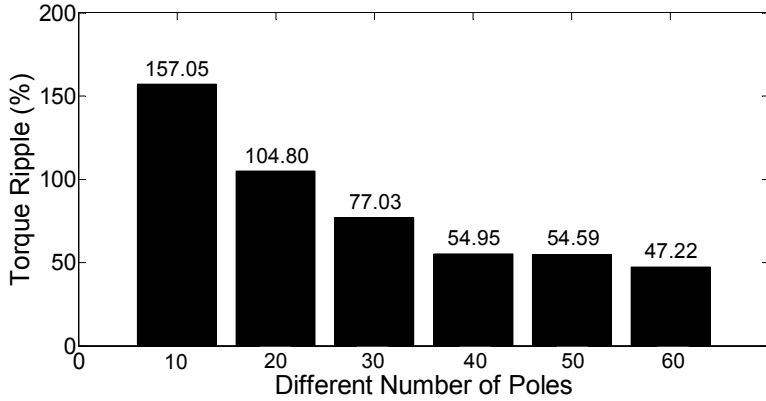
Fig. 7 – *Torque ripple percentage for different pole numbers at constant frequency.*

3.2 The influence of air gap length

Air gap is one of the most important factors in the performance of electrical machines. In the design process, there is always an attempt to choose the lowest possible air gap between the rotor and the stator along with consideration of both the mechanical constraints and the leakage flux limitations. In this section, the claw pole TFPM machine is redesigned for several air gap lengths while the rest of the structural parameters are kept constant and their internal voltages are also studied. Fig. 8 shows the internal voltage for different air gap lengths. It should be noted, only the air gap length has changed while the air gap's geometry construction does not change. As shown in Fig. 8, when the air gap length increases from 0.1 to 2.5 mm, voltage magnitude reduces and the internal voltage waveform is more close to sinusoidal waveform. The bar chart of torque ripple percentage for different air gap lengths is depicted Fig. 9. With increase of the air gap length, the torque ripple reduces as shown in this figure.
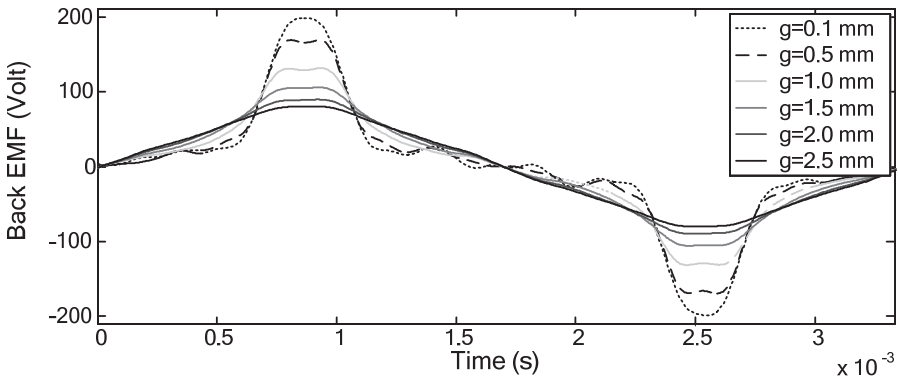

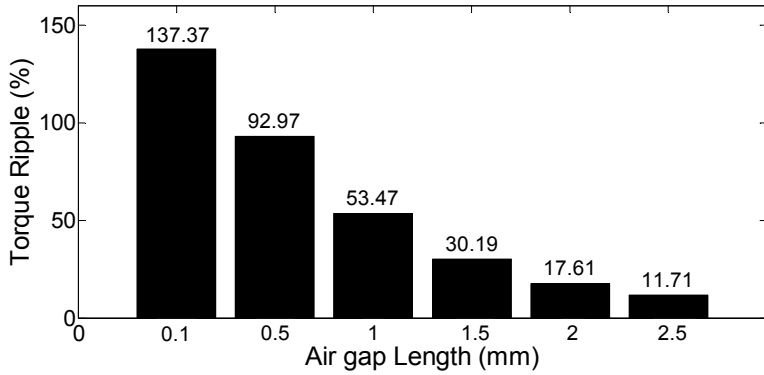Fig. 8 – *Internal voltage waveforms for different air gap lengths.*

Fig. 9 ─ *Torque ripple percentage for different air gap lengths.*

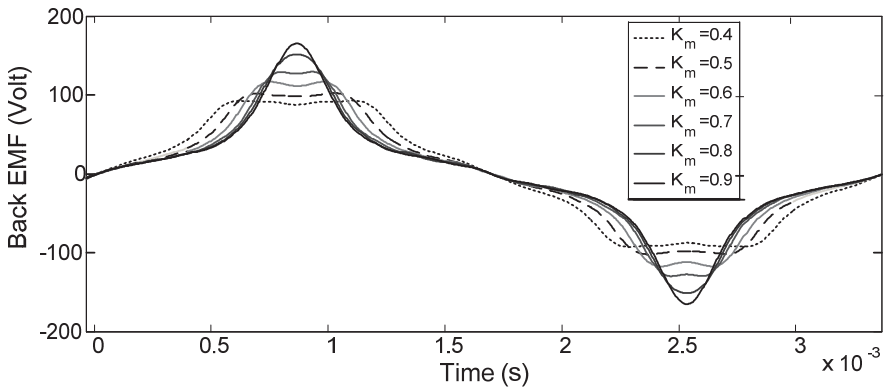## 3.3 The influence of magnet to flux concentrator ratio

Fig. 10 ─ *Internal voltage waveforms for different values of K_m.*
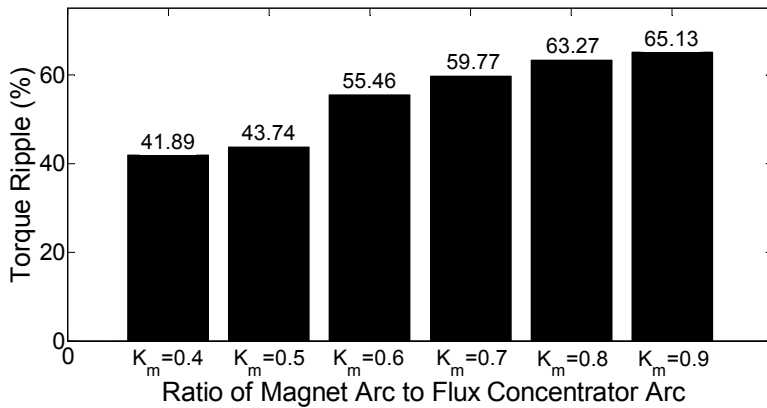

Fig. 11 ─ *Torque ripple percentage for different values of K_m.*

139

Ratio of circumferential length of the magnet to circumferential length of the flux concentrator of the rotor is defined as K_m. K_m significantly influences the machine performance as well as internal voltage waveform. As a result, torque ripple also changes. Internal voltage waveform for different values of K_m is depicted in Fig. 10. The bar chart of Torque ripple percentage for different values of K_m is also shown in Fig. 11. With increasing K_m from 0.4 to 0.9, the torque ripple increases from 41.89% to 65.13%.

3.4 The influence of stator pole shoes

The shape of the stator pole shoe is the shape of stator tooth surface adjacent to the air gap surface. This surface can be rectangular, triangular, trapezoidal, or other shapes. Different views of the stator tooth used in this paper are shown in Fig. 12.
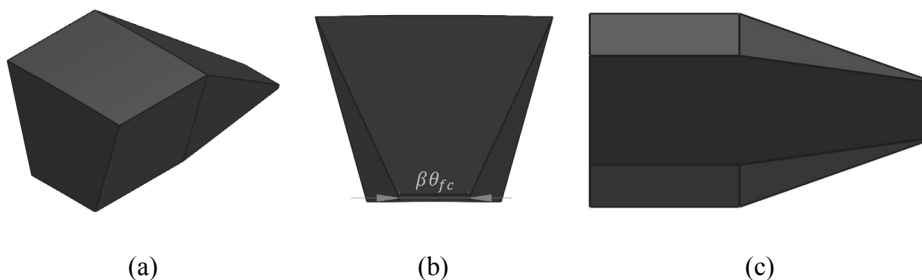
(a)   (b)   (c)

Fig. 12 – *Different views of the stator tooth:*
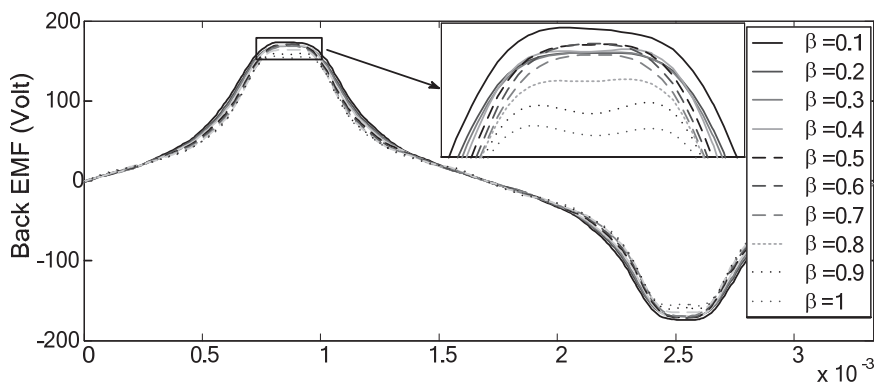(a) *3-D view*, (b) *Front view*, (c) *Bottom view*.

Fig. 13 – *Internal voltage waveforms for different shapes of pole shoe of stator.*

As is clear from the bottom-view the shape of stator tooth adjacent to the air gap surface, is trapezoidal. According to the front-view, the tip of the pole shoe covers only a part of the flux concentrator arc, which is determined by the coefficient of β, instead of its full coverage. The coefficient β could be

considered as the ratio of the arc of tip of the stator tooth surface adjacent to the air gap to the arc of flux concentrator. The effect of the stator pole shoe shape, by variation of the β value, on the internal voltage is shown in Fig. 13 where the internal peak voltages are depicted in more detail. According to this figure, internal voltage waveform is more close to sinusoidal waveform as β value is reduced. Although the internal voltage is not remarkably changed by variation of the β value, the torque ripple will be improved. Fig. 14 illustrates bar chart of the torque ripple percentage for different shapes of the pole shoe of the stator. Considering Fig. 14, the output torque ripple has increased by 22.26% when β value increases from 0.15 to 0.95.
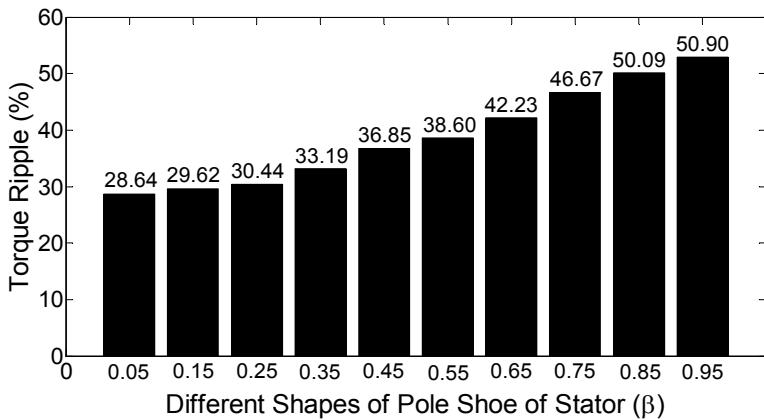

Fig. 14 – *Torque ripple percentage for different shapes of pole shoe of stator.*

3.5 The influence of coverage percentage by the stator teeth

In the previous subsection the effect of shape of the pole shoe of stator was analysed where the area of stator tooth surface adjacent to the air gap was kept constant. Here we investigate the effect of area of stator tooth surface adjacent to the air gap, while shape of the pole shoe of stator is kept unchanged. Ratio of the stator pole area to rotor pole area is the coverage is expressed by coefficient K_{co}. K_{co} considerably affects the shape of internal voltage waveform of the Claw pole TFPM machine. Also, the internal voltage rises as K_{co} increases. The internal voltage waveform for different values of K_{co} is shown in Fig. 15. According to this figure, the amplitude and rms of the internal voltage increases when K_{co} increases from 50% to 60% and then they drop for higher K_{co} values. However, the effect of K_{co} on the internal voltage harmonics is not noticeable. The bar chart of the torque ripple percentage, ratio of torque ripple to average torque, for different values of K_{co} are illustrated Fig. 16.

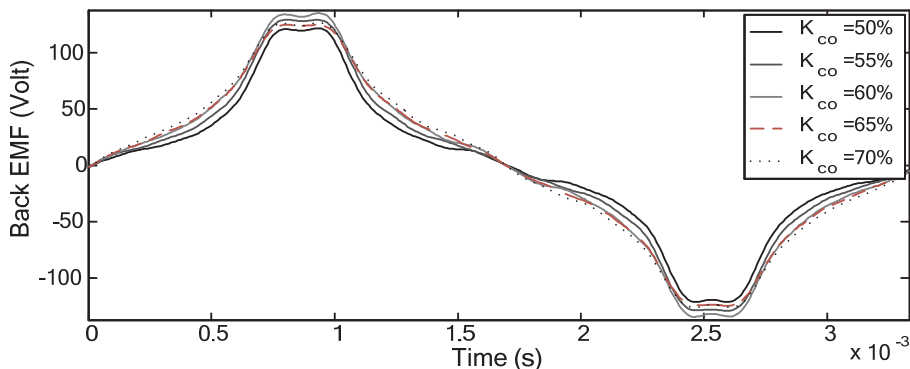Considering this figure, with increasing K_{co} from 50% to 70% the torque ripple decreases by 15.4%.

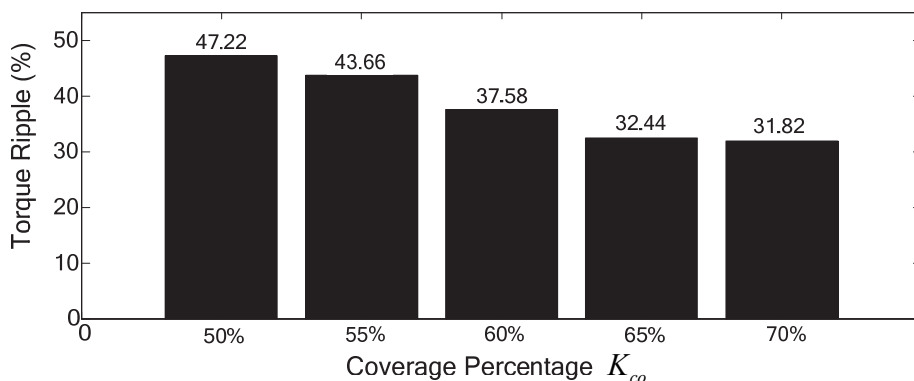**Fig. 15** – *Internal voltage waveforms for different values of K_{co}.*

Fig. 16 – *Torque ripple percentage for different values of K_{co}.*

4   Conclusion

In this paper, the structure and a number of sizing equations of Claw Pole Transverse Flux Permanent Magnet machines were presented. As a case study, a 500 kW, 300 rpm motor was designed. Effects of different structural factors on the internal voltage and electromagnetic torque ripples were investigated. It was found that by increasing the number of poles the internal voltage gets closer to a sinusoidal waveform and the torque ripple percentage is decreased. Increasing the air gap length improve both the internal voltage waveform and torque ripple. For low values of permanent magnet to flux concentrator ratios K_m, internal voltage waveform looks like a triangular waveform, whereas for higher values of K_m internal voltage waveform approaches to a trapezoidal waveform. Also, Increasing K_m decreases the torque ripple percentage. It was shown through simulations that the shape of stator pole shoe does not have a

dramatic effect on the shape of internal voltage, although it affects the torque ripple percentage. The influence of percentage of rotor coverage by the stator teeth K_{co} is negligible, but increasing this coefficient decreases the torque ripple percentage. The result presented in this paper gives a valuable insight to designers of Claw Pole TFPM Machines on how different parameters and structural factors of machine affect its performance. However, it seems that intelligent optimization methods, such as Genetic Algorithm, should be employed in order to obtain an optimized design of the machine.

4   References

[1]   A. Masmoudi, A. Elantably: An Approach to Sizing High Power Density TFPM Intended for Hybrid Bus Electric Propulsion Electric Machines and Power Systems, Vol. 28, No. 4, 2000, pp. 341 – 354.

[2]   J. F. Gieras: Permanent Magnet Motor Technology, Design and Applications, CRC Press, NY, USA, 2010.

[3]   M.R.J. Dubois: Optimized Permanent Magnet Generator Topologies for Direct-Drive Wind Turbines, PhD Thesis, Delft University of Technology, Delft, Netherlands, 2004.

[4]   Y.G. Guo, J.G. Zhu, P.A. Watterson, W. Wu: Development of a PM Transverse Flux Motor with Soft Magnetic Composite Core, IEEE Transaction on Energy Conversion, Vol. 21, No. 2, June 2006, pp. 426 – 434.

[5]   H. Weh, H. May: Achievable Force Densities for PM Excited Machines in New Configurations, International Conference on Electrical Machines, Munich, Germany, 08-10 Sept. 1986, pp. 1107 – 1111.

[6]   A. Masmoudi, A. Njeh, A. Elantably: On the Analysis and Reduction of the Cogging Torque of a Claw Pole Transverse Flux Permanent Magnet Machine, European Transactions on Electrical Power, Vol. 15, No. 6, Nov/Dec. 2005, pp. 513 – 526.

[7]   A. Masmoudi, A. Njeh, A. Mansouri, H. Trabelsi, A. Elantably: Optimizing the Overlap between the Stator Teeth of a Claw Pole Transverse-flux Permanent-magnet Machine, IEEE Transactions on Magnetics, Vol. 40, No. 3, May 2004, pp. 1573 – 1578.

[8]   P. Pillay, R. Krishnan: Modeling of Permanent Magnet Motor Drives, IEEE Transactions on Industrial Electronics, Vol. 35, No. 4, Nov. 1988, pp. 537 – 541.

[9]   R. Islam, I. Husain: Analytical Model for Predicting Noise and Vibration in Permanent-Magnet Synchronous Motors, IEEE Transactions on Industry Applications, Vol. 46, No. 6, Nov/Dec. 2010, pp. 2346 – 2354.

[10]   S. Huang, J. Luo, T.A. Lipo: Analysis and Evaluation of the Transverse Flux Circumferential Current Machine, IEEE Industry Applications Conference, New Orleans, LA, USA, 05-09 Oct. 1997, Vol. pp. 378 – 384.

[11]   JMAG Designer Online Help, Ver. 10.5, 2011.

[12]   S.T. Lundmark, E.S. Hamdi: Construction, Operation and Internal Design of a Claw-Pole Servo Motor, Electromotion Journal, April/June 2006, pp. 127 – 134.

[13]   E. Pinguey: On the Design and Construction of Modulated Pole Machines, PhD Thesis, Newcastle University, Newcastle upon Tyne, UK, 2010.